PHYSICAL REVIEW A VOLUME 24, NUMBER 5 NOVEMBER 1981

Two-photon ionization of H_2

Burke Ritchie
Sandia National Laboratories, Albuquerque, New Mexico 87185
and Department of Chemistry, University of Alabama, University, Alabama 35486

E. J. McGuire
Sandia National Laboratories, Albuquerque, New Mexico 87185
(Received 6 February 1981)

The nonresonant-multiphoton-ionization problem for a diatomic molecule is formulated as the one-photon ionization of a perturbed orbital. The continuum and perturbed orbitals are calculated in the "frozen-core" Hartree-Fock potential of the molecular ion. These orbitals are expanded in spherical harmonics about the internuclear center of mass, and the projected, coupled radial equations are solved iteratively. The radial perturbed orbitals are obtained in every iteration using an exact Green's function calculated in the diagonal, local elements of the potential matrix. This step is of some interest since use of the Green's function to achieve, implicitly, the summations over complete sets of intermediate states has previously been confined to Coulomb or quantum defect method modified-Coulomb problems.

I. INTRODUCTION

Owing to its small probability even at high photon fluxes, nonresonant multiphoton ionization (MPI) has been of limited experimental interest compared with resonant multiphoton ionization (RMPI). Recent work,[1] however, has defined conditions under which RMPI can be described by rate theory. The rate constants of this description can include those of nonresonant steps, an $(N-1)$-photon Rabi rate[2] or, if the resonant state requires n photons to be ionized, an n-photon ionization rate which is nonresonant when $n>1$, for example. $N+n-1$ is the total order of the ground-state ionization; thus, if $N>2$ or $n>1$, the Rabi rate for the bound-bound transition or the ionization rate for the bound-free transition, respectively, must be calculated using $(N-2)$-order or $(n-1)$-order perturbed states. Thus it is important to study theoretical methods for obtaining MPI cross sections, although, owing to their smallness, they may not be of direct experimental interest. For example, in the two-photon nonresonant ionization of H_2, the one-photon perturbed state (conceptualized as the virtual state to be ionized) is the same, within an energy shift, as the one-photon perturbed state (conceptualized as the virtual state to be excited) leading to three-photon resonant ionization of H_2 by excitation to an intermediate $^1\Sigma_g$ state.

There has been much work on the calculation of atomic MPI cross sections. It is well known that the summations over complete sets of intermediate states present the main difficulty. Green's functions have been used to achieve these summations implicitly. However, their use has been somewhat sparing, confined to Coulomb problems[3] or to modified-Coulomb problems based on the use[4] of the quantum defect method (QDM). Recently, McGuire[5] has derived an algorithm for constructing the exact Green's function for any radial potential which can be accurately represented according to a method published[6] by him some years ago and used extensively since then in atomic one-photon ionization problems. This method is of some interest since the large-r validity of the QDM modified-Coulomb Green's function[4] restricts its use to the alkali atoms or to excited states,[7,8] for which the appropriate amplitudes receive their greatest contributions from the large-r region of the perturbed and unperturbed orbitals. Ground-orbital ionization, however, requires the use of theoretical methods valid over the entire range of r. Perturbed orbitals [in dimensions of $a_0^{3/2}$ according to Eq. (1)] are plotted in Fig. 5 to illustrate the importance of small-r contributions to the two-photon radial amplitudes [Eq. (4c)].

II. THEORY

Theoretical studies of molecular MPI have been small in number. The study of Davidkin and Rapoport[8] on the two-photon ionization of excited H_2 demonstrates persuasively that the nuclear motion (requiring the explicit inclusion of vibrational-rotational states) is of minor importance far from resonances. Since the validity of the Born-Oppenheimer theorem depends on a much shorter orbital period for the electron than for the nuclei, we expect that nuclear motion will be negligible in the nonresonant two-photon ionization of the ground state. Thus the process is described as a vertical transition occurring at an internuclear distance of $1.4a_0$. The experimental vertical ionization potential is that for absorption of a 754-Å photon.[9] In the present calculation each photon is assigned an energy somewhat greater

than one-half of this ionization potential or 8.854 eV (ejection of 1.269-eV electrons). This photon energy is chosen so that the one-photon perturbed wave function used to calculate the ionization amplitude may also be used to calculate the dynamic polarizability of H_2 for comparison against an accurate calculation[10] available at 8.854 eV. This procedure provides a check on the accuracy of our methods used to calculate the perturbed orbital.

The wave function for the molecule perturbed by the radiation field is calculated from first-order perturbation theory; thus the two-photon amplitude [see Eq. (3a) below] is a result from standard second-order perturbation theory. The zeroth-order problem is assumed to be solved in the Hartree-Fock (HF) approximation for the molecule.[11] The total first-order function is written as a product of an HF orbital[11] ψ_0 (for one of the σ_g electrons of H_2) and a perturbed orbital ψ_1. This product is symmetrized such that the total first-order function is a singlet state. The perturbed orbital is obtained from the equation (in Rydberg units),

$$[\nabla^2 - U(\vec{r}) + (\epsilon_0 + \epsilon_p)]\psi_1(\vec{r}) = -2\hat{\rho}\cdot\vec{r}\,\psi_0(\vec{r}) , \tag{1}$$

where $\hat{\rho}$ is a unit vector in the direction of polarization of the photon, ϵ_0 (−1.18652 Ry) is the orbital energy[11] of ψ_0, and ϵ_p is the photon energy in Ry (8.854/13.605). U is the nonlocal potential (operator) derived by multiplying the two-electron first-order equation [whose approximate solution is $\psi_0(\vec{r}')\psi_1(\vec{r}) + \psi_1(\vec{r}')\psi_0(\vec{r})$] from the left by $\psi_0(\vec{r}')$ and integrating the result over $\vec{r}'$. The equation for the continuum orbital ψ_c is obtained from Eq. (1) by replacing $\epsilon_0 + \epsilon_p$ and k^2 and the right-hand side (rhs) by zero. k^2 is equal to $2\epsilon_p - P$ or 0.09328 Ry (for the vertical ionization potential $P = 1.2083$ Ry). Note that P is not very different from $-\epsilon_0$, such that the two-photon vertical ionization is not very different from the one-photon ionization of the perturbed orbital ψ_1, whose orbital energy is $\epsilon_0 + \epsilon_p$. The potential U is usually referred to as "frozen-core" HF. Previous work[12-16] on the one-photon ionization of H_2 has used the H_2^+ orbital (calculated at an internuclear distance of $1.4a_0$) in place of ψ_0 and the frozen-core approximation[12]; the differences in the cross section appear to be fairly small. The use of ψ_0 in Eq. (1) derives from the use of a HF zeroth-order approximation. Its use in the equation for ψ_c is based on the convenience of having only one potential U to describe the perturbed- and ejected-electron motion.

The following expansions[12-16] about the internuclear midpoint in a molecule-fixed frame have been used for ψ_0, ψ_1, and ψ_c,

$$\psi_0(\vec{r}) = \sum_{l_0=0,2,\cdots}^{\infty} \psi_{l_0 0}(r) Y_{l_0 0}(\theta_r, \phi_r) , \tag{2a}$$

$$\psi_1(\vec{r}) = \sum_{l_1 m_1} \psi_{l_1 m_1}(r) Y_{l_1 m_1}(\theta_r, \phi_r) Y^*_{1 m_1}(\theta_{\hat{\rho}}, \phi_{\hat{\rho}}) , \tag{2b}$$

$$\psi_c(\vec{r}, \vec{k}) = (4\pi) \sum_{l l' m_1 m_2} \psi^{(-)}_{l l' m_1+m_2}(r, k) Y_{l m_1+m_2} \times (\theta_r, \phi_r) Y^*_{l' m_1+m_2}(\theta_k, \phi_k) . \tag{2c}$$

The continuum partial waves [Eq. (2c)] are in general labeled by the indices ll' (for scattered-wave angular momentum states l and incident-wave angular momentum states l') and $m_c = m_1 + m_2$. The azimuthal index (in which the equations are uncoupled for linear molecules) is in general, equal to $m_I + m_2$, where m_I belongs to the perturbed orbital [Eq. (2b)] and m_2 to the dipole interaction of the perturbed orbital with the radiation field. For a $m_0 = 0$ (σ-type) initial orbital [Eq. (2a)], $m_I = m_1$, where m_1 belongs to the dipole interaction of the initial orbital with the radiation field. Equation (2c) has been discussed by Temkin *et al.*[17] for the e, H_2^+ scattering problem. Terms to order $l_0 = 4$ are sufficient to represent ψ_0 (as measured by the contributions to the cross section). The rhs of Eq. (1) causes terms to order $l_1 = 5$ to be generated; however, terms to order $l_1 = 3$ are retained, and the $l_1 = 1$ terms are observed to be dominant. This dominance limits l and l' to orders not greater than 2.

On averaging[17] over all orientations of the molecule-fixed frame (specified by the Euler angles $\alpha_0\beta_0\gamma_0$) relative to a space-fixed frame in which $\hat{\rho}$ and $\vec{k}$ (in the direction of ejection Ω) are defined, the two-photon ionization cross section is

$$\frac{d\sigma_2^{(m')}}{d\Omega} = (8\pi^2)^{-1} \int_0^{2\pi} d\alpha_0 \int_0^{\pi} \sin\beta_0 d\beta_0 \int_0^{2\pi} d\gamma_0 \left[\frac{\alpha a_0^2 k \epsilon_p}{4\pi} \left(\frac{I}{I_0}\right) \left| \langle \psi^{(-)}_{\vec{k}}(\vec{r}) | \rho\cdot\vec{r} | \psi_1(\vec{r}) \rangle \right|^2 \right], \tag{3a}$$

$$\frac{d\sigma_2^{(m')}}{d\Omega} = \frac{\sigma_2^{(m')}}{4\pi} [1 + \beta_2 P_2(\cos\theta) + \gamma_2 P_4(\cos\theta)] . \tag{3b}$$

The coefficients of $P_L(\cos\theta)$ are $b_L^{(m')} = \sigma_2^{(m')}/4\pi$ for $L = 0$, $b_2^{(m')} = \sigma_2^{(m')}\beta_2/4\pi$ for $L = 2$, and $b_4^{(m')} = \sigma_2^{(m')}\gamma_2/4\pi$ for $L = 4$. Generally,

$$b_L^{(m')} = 2\alpha a_0^2 k \epsilon_\rho \left(\frac{I}{I_0}\right) \sum S^{(m')}(l_\rho \lambda_\rho m_1 \mu_1 m_2 \mu_2)(2l'+1)^{1/2}(2\lambda'+1)^{1/2}(2L+1)$$
$$\times \begin{pmatrix} l_\rho & \lambda_\rho & L \\ 2m' & -2m' & 0 \end{pmatrix} \begin{pmatrix} l_\rho & \lambda_\rho & L \\ (m_1+m_2) & -(\mu_1+\mu_2) & -(m_1+m_2-\mu_1-\mu_2) \end{pmatrix} \begin{pmatrix} l' & \lambda' & L \\ 0 & 0 & 0 \end{pmatrix}$$
$$\times \begin{pmatrix} l' & \lambda' & L \\ (m_1+m_2) & -(\mu_1+\mu_2) & -(m_1+m_2-\mu_1-\mu_2) \end{pmatrix} (a_{\lambda'\lambda\lambda_1\mu_1\mu_2})^* a_{l'll_1m_1m_2}, \tag{4a}$$

$$S^{(m')}(l_\rho \lambda_\rho m_1 \mu_1 m_2 \mu_2) = (-1)^{m_1+m_2+\mu_1+\mu_2}(2l_\rho+1)(2\lambda_\rho+1)$$
$$\times \begin{pmatrix} 1 & 1 & l_\rho \\ m_1 & m_2 & -(m_1+m_2) \end{pmatrix} \begin{pmatrix} 1 & 1 & \lambda_\rho \\ \mu_1 & \mu_2 & -(\mu_1+\mu_2) \end{pmatrix} \begin{pmatrix} 1 & 1 & l_\rho \\ m' & m' & -2m' \end{pmatrix} \begin{pmatrix} 1 & 1 & \lambda_\rho \\ m' & m' & -2m' \end{pmatrix}, \tag{4b}$$

$$a_{l'll_1m_1m_2} = (-1)^{m_1+m_2} \left(\frac{3}{4\pi}\right)^{1/2} (2l_1+1)^{1/2}(2l+1)^{1/2} \begin{pmatrix} l_1 & 1 & l \\ 0 & 0 & 0 \end{pmatrix} \begin{pmatrix} l_1 & 1 & l \\ m_1 & m_2 & -(m_1+m_2) \end{pmatrix}$$
$$\times \int_0^\infty dr\, r^2 \psi^{(-)*}_{ll'm_1+m_2}(r,k) r \psi_{l_1m_1}(r), \tag{4c}$$

where $m'=0$ for linear polarization and $m'=\pm 1$ for left or right circular polarization, α is the fine-structure constant, a_0 the Bohr radius, I the radiation intensity in W cm^{-2}, and $I_0 = 14.038 \times 10^6$ W cm^{-2}. For $m'=0$ θ is the angle between $\hat{\rho}$ and $\hat{k}$, and for $m'=\pm 1$ it is the angle relative to the photon propagation direction (perpendicular to $\hat{\rho}$). Equations (3b) and (4) were derived by defining the dipole amplitude in Eq. (3a) in a molecule-fixed coordinate frame and then by expressing the photon polarization vectors and ejected-electron spherical harmonics [see Eq. (2c)] in terms of their rotational transforms in a laboratory-fixed coordinate frame using the rotational harmonics $D^{(j)}_{m_j m_j}(\alpha_0 \beta_0 \gamma_0)$. These rotational transformations are standard in electron-molecule theory in which scattering or photoionization cross sections are averaged over molecular orientations.[17] The summation in Eq. (4a) runs over all indices (except m') consistent with parity conservation. All summation indices except l_ρ, λ_ρ, and L are defined by Eqs. (2) ($l_0 l_1 l l' m_1 m_2$) and their conplex conjugates ($\lambda_0 \lambda_1 \lambda \lambda' \mu_1 \mu_2$). The indices l_ρ and λ_ρ derive from the additions of angular momenta implicit in Eq. (4b), and L [order of $P_L(\cos\theta)$] derives from the additions of angular momenta implicit in Eq. (4a).

The correctness of this result has been checked by deriving the coefficients of the products of radial matrix elements [see Eq. (4c)] in the spherical-atom limit ($l=l'=0$ or 2; $l_1=1$, $l_0=0$, and all elements equal for different values of m_1 and m_2). For $m'=0$ the coefficients $b_0^{(0)}$, $b_2^{(0)}$, and $b_4^{(0)}$, when each is multiplied by $4\pi/9$ to account for the radial-matrix-element dependence on our definition [Eq. (2b)], agree with those which can be deduced from a formula given by Zernik.[18] In Eq. (4a) the factor 2 is the occupation number of the σ_g orbital.

TABLE I. Phase shifts $\eta_{ll'm}$. Numbers in parentheses are exponents.

		Uncoupled results		
Iteration	η_{000}	η_{220}	η_{221}	η_{222}
0	−1.510(−3)	6.541(−2)	3.492(−2)	−3.129(−2)
1	−0.4613	4.998(−2)	2.005(−2)	−4.464(−2)
2	−0.4772	3.030(−2)	3.228(−2)	−5.616(−2)
3	−0.4737	2.883(−2)	1.847(−2)	−5.698(−2)
		Coupled results		
Iteration	η_{000}	η_{020}	η_{200}	η_{220}
0	6.866(−2)	−3.750(−3)	−3.750(−3)	5.949(−2)
1	−0.3755	1.003(−2)	0.1124	4.033(−2)
2	−0.3915	1.129(−2)	2.328(−2)	2.336(−2)
3	−0.3885	1.109(−2)	1.113(−2)	2.226(−2)

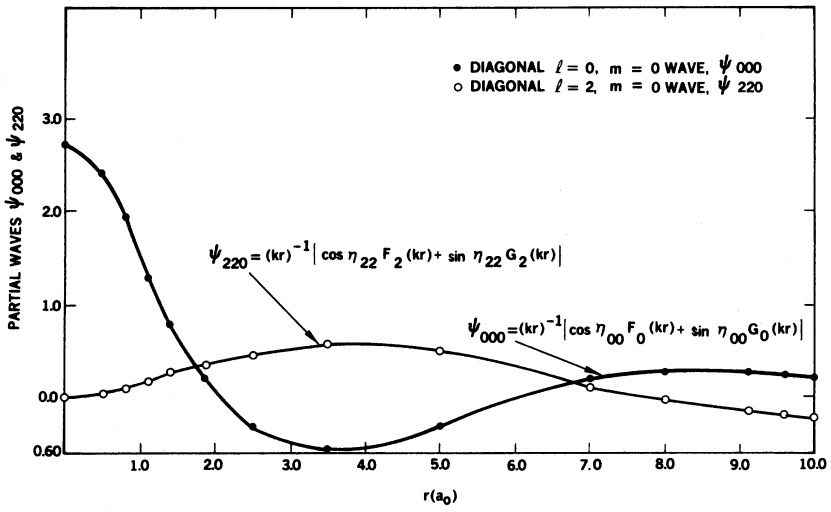

FIG. 1. Diagonal partial waves versus r.

III. NUMERICAL METHODS AND RESULTS

Owing to the complexity of the radial equations they are not presented here. The methods used to obtain the continuum partial waves $\psi^{(-)}_{ll'm}(r,k)$, normalized for incoming boundary conditions, have been described previously.[16] In the present work, however, the $l=0,2$ (rather than the $l=1,3$) coupled, radial integral equations[19] are solved iteratively (rather than noniteratively as in Ref. 16) with respect to the nonlocal exchange terms of U. Their convergence, as measured by the change in the phase shifts with iteration (Table I), is rapid. From Table I note that the equality (i.e., K-matrix symmetry) of the nondiagonal phase shifts is used as a measure of the convergence. Figures 1–3 show the diagonal and nondiagonal waves used in the calculation, with their appropriate large-r limiting expressions. Coupling in the continuum affects the two-photon ionization results by less than a few percent. Figures 2 and 3 show that the nondiagonal waves have appreciable amplitudes at small r. These lead to dipole-amplitudes [with $\psi_{1m_l}(r)$, Fig. 5] whose magnitude is significant; however, their effect of the cross section (Fig. 6) is small owing to the largeness of the dipole amplitudes belonging

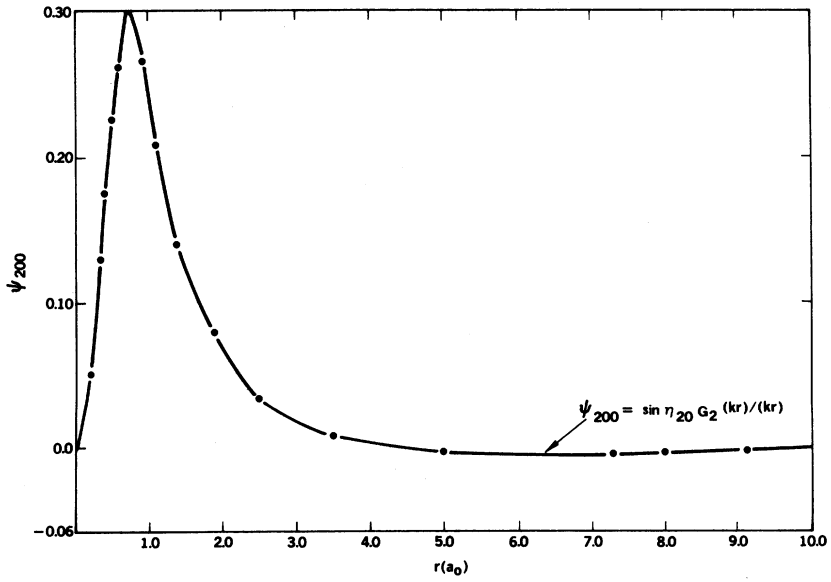

FIG. 2. Nondiagonal partial wave versus r.

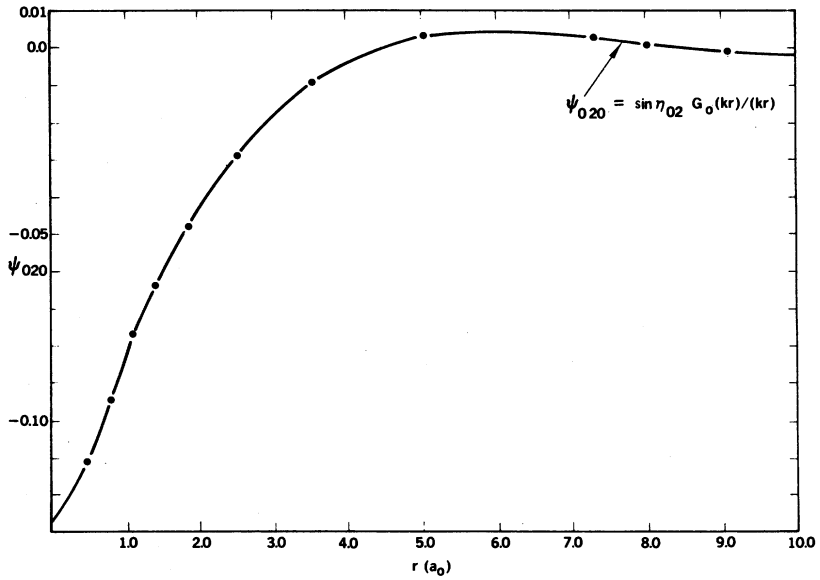

FIG. 3. Nondiagonal partial wave versus r.

to the diagonal waves. In previous work[16] it was found that partial cross sections for ionization with rotational excitation of the molecular ion depend strongly on the nondiagonal dipole amplitudes for 1,3 coupling. This happens because the large dipole amplitudes combine in a way that they nearly cancel, thus reducing their contribution to a value comparable to that of the much smaller nondiagonal dipole amplitudes.

The coupled, inhomogeneous radial equations from Eq. (1) were also solved iteratively. These iterations are made both with respect to the nonlocal exchange terms and to the $l_1 = 1,3$ coupling terms. The zeroth-order, uncoupled equations contain only the local radial potentials $u_{l_1 l_1 m_1}(r)$, which are the diagonal matrix elements of the local part of $U(r)$ in Eq. (1) in the spherical-harmonics basis. These equations have radial inhomogeneities $\rho_{l_1 m_1}(r)$ appropriate for a given $l_1 m_1$ projected equation. The rhs of Eq. (1) does not cause the radial perturbed orbitals to be coupled. The $l_0 > 0$ components of ψ_0, however, cause $l_1 > 1$ inhomogeneous terms to be generated. The $l_0 > 0$ terms depend on m_1, i.e., there are distinct radiative perturbations on ψ_0 for $m_1 = 0$ (molecular axis parallel to the photon polarization in the molecule-fixed or rotating frame) and $m_1 = \pm 1$ (molecular axis perpendicular to the photon polarization in the molecule-fixed frame). The expansion for ψ_0 [Eq. (2a)] converges rapidly as measured by the relative strengths of the $\rho_{l_1 m_1}(r)$ terms over their entire range of r. For example, the $\rho_{3m_1}(r)$ terms are sufficiently small that the $\psi_{3m_1}(r)$ perturbed orbitals have small amplitudes relative to those of $\psi_1 m_1(r)$ (Fig. 5). The use of the small orbitals produces changes of less than a few percent in the ionization cross section (Fig. 6) and polarizabilities (Fig. 4). Perturbed orbitals for $l_1 > 3$ are neglected (as are $l_0 > 4$ components of ψ_0). In going to larger molecules this convergence is expected to be much slower. However, the number of components in an outer-shell ψ_0 which can cause large-amplitude perturbed orbitals (such as those in Fig. 5) may still be fairly small. The convergence of ψ_0 and in the continuum has been studied previously[20] on the one-photon ionization of CO.

The perturbed radial orbitals $\psi_{l_1 m_1}(r)$ are obtained by calculating the Green's functions[5] defined by the equations,

$$\left(\nabla_r^2 - \frac{l_1(l_1+1)}{r^2} - u_{l_1 l_1 m_1}(r) + (\epsilon_0 + \epsilon_p)\right) G_{l_1 m_1}(r, r'; \epsilon_0 + \epsilon_p) = \frac{\delta(r - r')}{rr'}, \quad (5a)$$

$$\nabla_r^2 = \frac{d^2}{dr^2} + \frac{2}{r}\frac{d}{dr}. \quad (5b)$$

The details of this step are given in the Appendix. These Green's functions are used repeatedly in iterations with respect to all (diagonal and nondiagonal) nonlocal exchange terms and with respect to the nondiagaonal elements of the local part of U. In the first and subsequent iterations these contributions occur as extra inhomogeneities added to $\rho_{l_1 m_1}(r)$.

The convergence is studied in Fig. 4 for the isotropic and anisotropic parts of the dynamic polar-

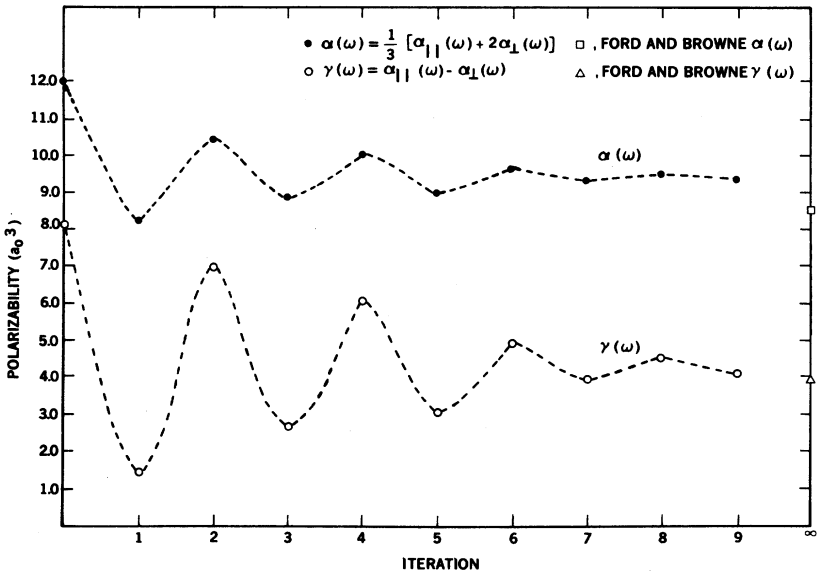

FIG. 4. Convergence of the H_2 polarizability.

izability of H_2, $\alpha(\omega)=\frac{1}{3}[\alpha_{\parallel}(\omega)+2\alpha_{\perp}(\omega)]$ and $\gamma(\omega)=\alpha_{\parallel}(\omega)-\alpha_{\perp}(\omega)$, respectively. The parallel ($\alpha_{\parallel}$) and perpendicular ($\alpha_{\perp}$) components are calculated using perturbed orbitals for $m_1=0$ and $m_1=\pm1$, respectively. This calculation is performed at the same photon energy (8.854 eV) used in the ionization calculation. Further, the polarizability is defined[10] such that Eq. (1) [and Eq. (5a)] must also be solved at the energy $\epsilon_0-\epsilon_p$. In Fig. 4 our results are observed to converge after nine iterations to within about 10% for $\alpha(\omega)$ and about 4% for $\gamma(\omega)$ of the accurate values of Ford and Browne.[10] The remaining discrepancy probably derives from the one-electron model used in the present work.

The oscillatory convergence is the result of the dominance of the diagonal exchange terms in the corrections to the zeroth-order solution. These are repulsive (for singlet symmetry) at the energy studied [at which the perturbed orbitals (Fig. 5) are positive]. The radial parts of the dipole-interaction terms $\rho_{l_1 m_1}(r)$ are positive; thus the rhs

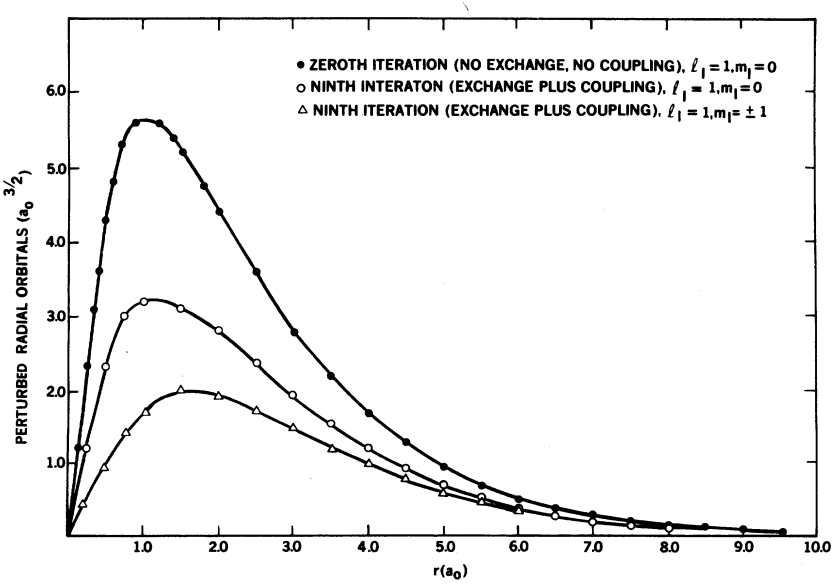

FIG. 5. Zeroth-iteration perturbed orbital ($l_1=1$, $m_1=0$) and ninth-iteration perturbed orbitals ($l_1=1$, $m_1=0$ and $l_1=1$, $m_1=\pm1$) versus r.

of Eq. (1) is negative and is responsible for the large positive amplitude in the zeroth-order iteration (Fig. 5) since the Green's functions are negative at this energy. Thus the first-iteration estimate of the repulsive exchange terms is too large since the amplitudes of the zeroth-order perturbed orbitals are too large. Since these overestimated terms are added to the netative dipole-interaction terms, the first-iteration rhs is raised to less negative values than the zeroth-order rhs. This rhs is too small in magnitude, however, so that the first-iteration perturbed orbitals give the low polarizabilities (Fig. 4) and underestimate the exchange terms for the second iteration. This process is cyclic; thus the even-order iterations converge monotonically from above, while the odd-order iterations converge monotonically from below the accurate polarizabilities. Although the nondiagonal, local potentials $u_{13m_1}(r)$ are as attractive at r values close to one-half the internuclear distance as the diagonal, local potentials $u_{11m_1}(r)$ and $u_{33m_1}(r)$, the coupling between the $l_1=1$ and $l_1=3$ perturbed orbitals is of minor importance. (Note that there are also coupling terms in the nonlocal, exchange part of the potential, and these are also of minor importance.) The main reason for the unimportance of coupling appears to be the small dipole-interaction rhs's for the $l_1=3$ equations, causing small-amplitude perturbed orbitals $\psi_{3m_1}(r)$. The leading term of $\rho_{3m_1}(r)$ depends on the quadrupolar component of l_0, which is small for H_2. A contributing factor to the weak coupling (which plays the major role in the homogeneous continuum equation) is the larger strength of the centrifugal barrier for higher-l_1 orbitals relative to the strengths of low-Z coupling terms in the potentials.

The two-photon angular distributions and their parameters are shown in Fig. 6. They are presented for linearly ($m'=0$) and circularly ($m'=\pm1$) polarized photons. The ratio of the total cross sections (σ_2) for linear to circular polarization is 1.34. According to theory the maximum ratio[21,22] is 1.5.

These results are for the ninth-iteration 1,3-coupled perturbed orbitals discussed above. They are presented for coupled and uncoupled 0,2 partial waves (Figs. 1–3 and Table I). The continuum wave function has been orthogonalized to ψ_0; however, this correction changes the results by less than a few percent.

The largest effect of the molecular field is caused by the dependence of the perturbed orbitals on m_1 and m_2. Spherical initial-state two-photon ionization results are simulated by setting all matrix elements equal to the matrix elements for $l_1=1$, $m_I=m_1=0\rightarrow l=0,2$ (uncoupled), $m=m_1+m_2=0$ (largest cross section in Fig. 6), *or* to the matrix elements for $l_1=1$, $m_I=m_1=1\rightarrow l=0,2$ (uncoupled), $m=m_1+m_2=1$ (smallest cross sec-

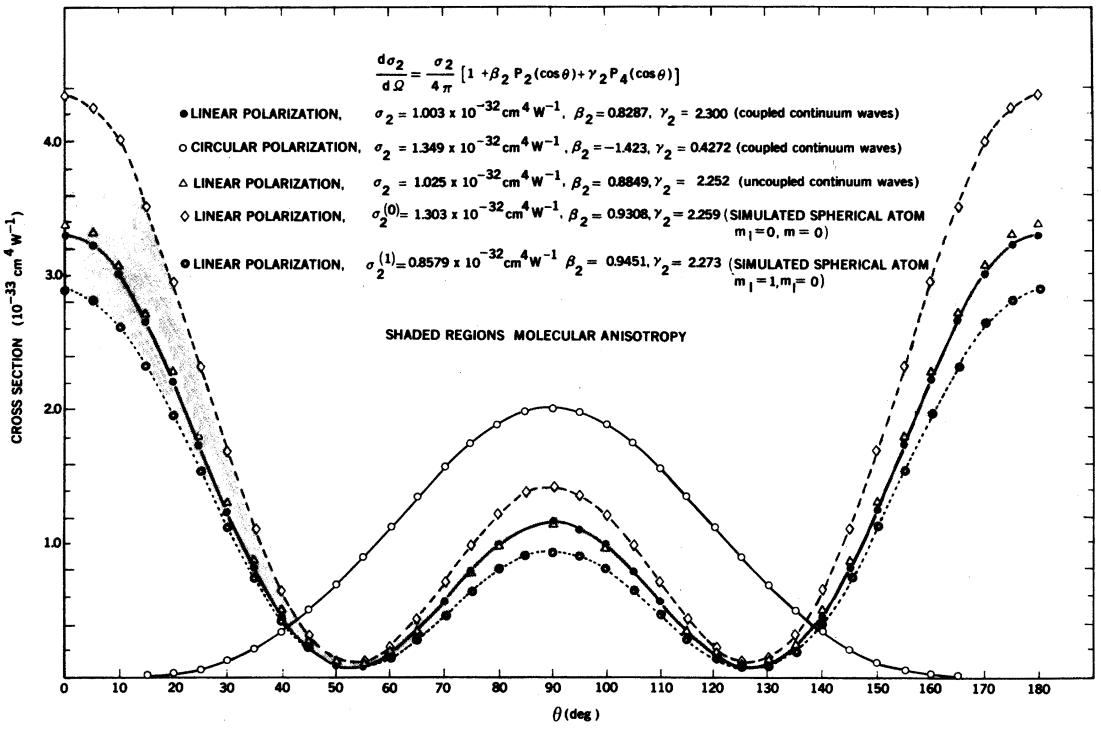

FIG. 6. Two-photon angular distributions and their parameters.

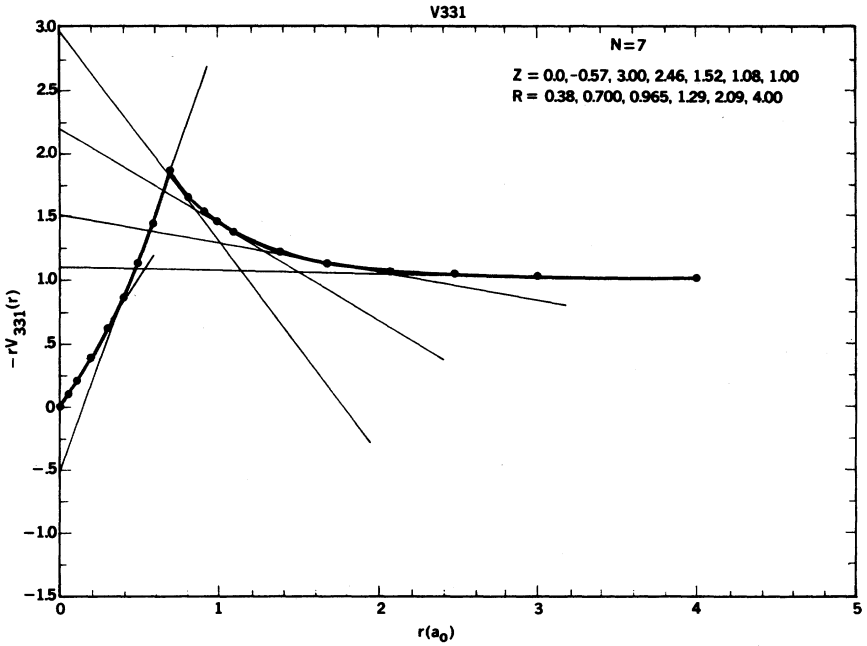

FIG. 7. Approximation of $-rV_{331}(r)$ (solid circles) by a sequence of straight-line segments.

tion of Fig. 6). The relative differences in the simulated and accurate results are a measure of the effect of molecular anisotropy on the cross section. In Fig. 6 the region between the dashed and dotted curves indicates the relative differences.

In conclusion, the total two-photon cross section ($m'=0$), $\sigma_2 = 1.003\times10^{-32}$ cm^4 W^{-1}, is about 20 times larger than that for the He atom.[23] It is about one-half as large as that for the H atom[24] per electron (i.e., once the H_2 cross section is scaled by one-half its value).

This work was supported by the U. S. Department of Energy.

APPENDIX

The various effective potentials $V_{ijK}(r)$ in the calculation were used to plot $-rV_{ijK}(r)$. In Fig. 7 $-rV_{331}(r)$ is shown as solid circles. Then $-rV_{ijK}(r)$ was approximated by a series of straight-line segments (seven in Fig. 7). That is, we used

$$V_{ijJ}(r) = -2Z_i/r + \Delta_i, \quad 1 \le i \le N \tag{A1}$$

with

$$2Z_i/r_i - \Delta_i = 2Z_{i+1}/r_i - \Delta_{i+1}$$

and $\Delta_N = 0$.

For these potentials the Green's function was obtained as in Ref. 5. The potentials used here are somewhat more complicated and we describe the special functions used in different regions of r. The radial Green's function is written $g_l(r,r') = h_l(r,r')/r$ and $h_l(r,r')$ satisfies

$$\frac{d^2}{dr^2}h_l(r,r') - \frac{l(l+1)}{r^2}h_l(r,r') + \left(2\frac{Z_i}{r} + (E-\Delta)\right)h_l(r,r') = \frac{\delta(r-r')}{r}. \tag{A2}$$

1. For $Z_i = 0$.

(a) With $E-\Delta>0$, and $a=(E-\Delta)^{1/2}$ we used $\phi^+ = arj_l(ar)$ and $\phi^- = (-1)^{l+1}arn_l(ar)$.

(b) With $E-\Delta<0$, and $\gamma=(-(E-\Delta)]^{1/2}$ we used $\phi_l^+ = e^{i\pi l/2}\gamma r j_l(i\gamma r)$ and $\phi_l^- = e^{i\pi(l+1)/2}\gamma r n_l(i\gamma r)$, where plus and minus refer to the regular and irregular solutions, which in this case are spherical Bessel functions.

2. For $Z_i > 0$.

(a) With $E-\Delta_i<0$ and $\gamma_i = Z_i/(\Delta_i - E)^{1/2}$ we used $\phi^+ = M_{\gamma_i, l+1/2}(2rZ_i/\gamma_i)$ and $\phi^- = W_{\gamma_i, l+1/2}(2rZ_i/\gamma_i)$, where M and W are standard[25] regular and irregular Whittaker functions and were used in Ref. 5.

(b) With $E-\Delta>0$ and $a_i = iZ_i/(E-\Delta_i)^{1/2}$ we used $\phi^+ = G_l(2rZ, -1/a^2)$ and $\phi^- = H_l'(2rz, -1/a^2)$ where G and H_l' are Hartree[25] functions defined by

$$G_l(2rZ, -1/a^2) = (-ia^2)^{l+1}M_{ia,l+1/2}(2rZ/ia)/\Gamma(2l+2)$$

and

$$i\sinh(\pi a)H_l'(2rZ,-1/a^2)=(-ia)^{l+1}W_{ia,l+1/2}(2rZ/ia)/\Gamma(l+1+ia)-e^{\pi a}G_l(2rZ,-1/a^2)\,.$$

With these definitions the Hartree functions, and all those used so far in defining ϕ^+ and ϕ^-, are real.

3. $Z_i<0$. To obtain real regular and irregular functions we modify the definitions from those used in case 2. That is,

(a) For $E-\Delta<0$ and $\gamma_i=Z_i/(\Delta_i-E)^{1/2}$ we used $\phi^+=M_{\gamma,l+1/2}(-2rZ/\gamma)$,

but

$$\phi^-=W_{\gamma,l+1/2}(-2rZ/\gamma)-i\pi M_{\gamma,l+1/2}(-2rZ/\gamma)/\Gamma((-l-\gamma)\Gamma(2l+2))\,.$$

(b) With $E-\Delta>0$ and $a_i=Z_i/(E-\Delta_i)^{1/2}$ we used $\phi^+=G_l'(-2rZ,-1/a^2)$ and $\phi^-=H_l''(-2rZ,-1/a^2)$,

with

$$G_l'(-2rZ,-1/a^2)=(ia)^{l+1}M_{ia,l+1/2}(-2rZ/ia)/\Gamma(2l+2)$$

and

$$i\sinh(\pi a)H_l''(-2rZ,-1/a^2)=(-ia)^{l+1}W_{ia,l+1/2}(-2rZ/ia)/\Gamma(l+1+ia)-e^{-\pi a}G_l(-2rZ,-1/a^2)/2\,.$$

These modifications arise from the log term in the definition[25]

$$W_{K,M}(X)=(-1)^{2M+1}M_{K,M}(X)\ln(X)/\Gamma(\tfrac{1}{2}-M-K)\Gamma(1+2M)+\cdots,$$

which leads to a complex function for X negative, and that we desire real functions in the Green's function.

[1]J. H. Eberly and S. V. ONeil, Phys. Rev. A 19, 1161 (1979), and references therein.

[2]For example, see B. Ritchie, Phys. Rev. Lett. 43, 1380 (1979).

[3]A. Maquet, Phys. Rev. A 15, 1088 (1977).

[4]B. A. Zon, N. L. Manakov, and L. P. Rapoport, Dok. Akad. Nauk. SSSR 188, 560 (1969) [Sov. Phys. Dokl. 14, 904 (1970)].

[5]E. J. McGuire, Phys. Rev. A 23, 186 (1981).

[6]E. J. McGuire, Phys. Rev. 175, 20 (1968).

[7]B. A. Zon, N. L. Manakov, and L. P. Rapoport, Zh. Eksp. Teor. Fiz. 61, 968 (1971) [Sov. Phys.—JETP 34, 515 (1972)].

[8]V. A. Davidkin and L. P. Rapoport, Kvant. Elektron. (Moscow) 2, 343 (1975) [Sov. J. Quantum Electron. 5, 195 (1975)].

[9]G. R. Cook and P. H. Metzger, J. Op. Soc. Am. 54, 968 (1964).

[10]A. L. Ford and J. C. Browne, Phys. Rev. A 7, 418 (1973).

[11]W. Kolos and C. Roothaan, Rev. Mod. Phys. 32, 205 (1960).

[12]W. D. Robb and L. A. Collins, Phys. Rev. A 22, 2474 (1980).

[13]H. P. Kelly, Chem. Phys. Lett. 20, 547 (1973).

[14]B. Ritchie, J. Chem. Phys. 63, 1351 (1975).

[15]C. M. Dutta, F. M. Chapman, and E. F. Hayes, J. Chem. Phys. 67, 1904 (1977).

[16]B. Ritchie and B. R. Tambe, J. Chem. Phys. 68, 755 (1978).

[17]A. Temkin, K. V. Vasavada, E. S. Chang, and A. Silver, Phys. Rev. 186, 57 (1979).

[18]W. Zernik, Phys. Rev. 135, A51 (1964).

[19]E. R. Smith and R. J. W. Henry, Phys. Rev. A 7, 1585 (1973).

[20]B. Ritchie and B. R. Tambe, J. Phys. B 13, L225 (1980).

[21]P. Lambropoulos, Phys. Rev. Lett. 28, 585 (1972).

[22]S. Klarsfelt and A. Maquet, Phys. Rev. Lett. 29, 79 (1972).

[23]B. Ritchie, Phys. Rev. A 16, 2080 (1977), and references therein.

[24]L. J. Slater, *Confluent Hypergeometric Functions* (Cambridge University Press, London, 1960).

[25]D. R. Hartree, Proc. Cambridge Philos. Soc. 24, 426 (1928).